

Achieving Electrical–Thermal Coupling in an Induction Motor Drive Model to Enhance Reliability of Sliding Mode based Controllers

Hamza Ahmad, Ki-Bum Park

Korea Advanced Institute of Science and Technology (KAIST), South Korea

ABSTRACT

Hardware in the loop Simulation (HILS) is a tool used for testing and validating real controllers with a real-time virtual plant. However, the fidelity of plant being modelled in HILS determines the reliability of the tested controller. In this paper, an induction motor drive is developed in HILS. Both Cauer and Foster thermal networks are employed for thermal and loss modelling of three phase rectifier, inverter, and induction machine. The developed model is used to test Integral Super-Twisting Sliding Mode Control (ISTSMC) scheme. ISTSMC is robust to internal perturbations and external disturbances and eliminates the chattering phenomenon which is associated with other sliding mode-based control strategies. The ISTSMC controller is built in a rapid-control prototyping device and is interfaced with HILS device. The results show that ISTSMC controller increases robustness of the system without adding thermal stresses to it.

1. Introduction

Testing control algorithm with real hardware prototypes poses challenges like safety, difficulty of testing protection concepts under fault conditions, prototype development costs. HIL testing of controllers in real-time, accounts for communication delays, and allows wide test coverage with high fidelity virtual prototype of the plant [1]. The effects of a control scheme on the thermal stresses of semiconductor junction are of great significance to evaluate its robustness [2]. Sliding mode control (SMC) is variable structure control and is robust to external disturbances and internal perturbations [3]. The SMC has inherent problem of chattering and thus can deteriorate the performance of drive system by incorporating thermal stress on the inverters. Thus, to improve the thermal performance and ensure smooth operation of electric drive system, ISTSMC is proposed, and its effectiveness validated with real-time HIL emulation.

2. Virtual Prototype Development

The plant is developed in Typhoon HIL real-time simulator, which consists of an FPGA, based multi-core solver with high-fidelity converters and machine models optimized for real-time simulation. The plant consists of an electrical domain model coupled with a thermal model. The ISTSMC controller is built in Imperix B-Box RCP and is interfaced with the HIL Device.

2.1 Electrical Domain Model

The electrical model of the variable speed drive consists of a diode rectifier, a DC link, a braking chopper, and an inverter. The induction motor is modelled as “voltage behind reactance”, which provides better numerical stability.

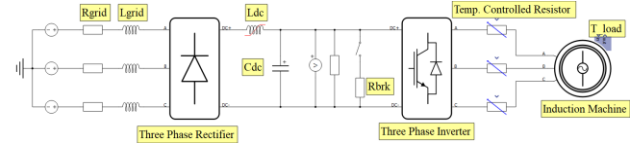


Fig. 1. Plant model developed in HIL based virtual environment.

Table. 1. Model Parameters

IM Parameters	Values	Parameters	Values
p	2	V_{dc}	800
R_s	0.76 Ω	f_s	10 kHz
R_r	0.44 Ω	t_d	1us
L_m	0.100 H	Rgrid	1 m Ω
L_r	0.0034 H	Lgrid	0.1 mH
L_s	0.0034 H	Ldc	1.5 mH
J	0.1 kg.m ²	Cdc	500 uF
C_{thm}	0.014 K/W	Rbrk	65 Ω
R_{thm}	3700 Ws/W

2.2 Electrical–Thermal Coupling

The thermal and power loss models of the diode rectifier, inverter and the induction machine are included. The switching and conduction losses are modelled as a function of voltage, current and temperature in terms of 3D look-up tables imported from datasheets. The losses calculated from foster model based, internally generated thermal network is fed to the heatsink which is a Cauer model based thermal network. The Cauer model represents all the material layers in a physical system with each layer modelled as thermal resistance $R_{thermal}$ and capacitance $C_{thermal}$ [4]. τ in (1) is the thermal constant. The thermal energy Q_{12} is transferred between layers is described in (2) where T_{12} is the temperature difference between two layers. Lastly, the thermal energy transferred Q_1 through capacitance is given by (3) which depends upon the change in temperature at point 1. In the case of induction machine’s thermal model, the effects of temperature on stator resistance are modelled. The model takes the stator currents along with ambient temperature and outputs motor temperature as well as changes in the stator resistance. Variable resistance is used to achieve the electrical–thermal coupling of the motor.

$$C_{thermal} = \frac{\tau}{R_{thermal}} \quad (1)$$

$$Q_{12} = \frac{T_{12}}{R_{thermal}} \quad (2)$$

$$Q_1 = C_{thermal} \frac{dT_1}{dt} \quad (3)$$

2.3 Integral Super Twisting Sliding Mode Control

To derive the mathematical expression for the proposed control scheme, the dynamic model of IM is used and given as follows:

$$\begin{cases} \frac{d}{dt} i_\alpha = -\left(\frac{L_m^2 \alpha_r + L_r R_s}{\varepsilon L_m}\right) i_\alpha + p \omega_r \varphi_\beta + \frac{L_r}{L_m} V_{s\alpha} + \alpha_r \varphi_\alpha \\ \frac{d}{dt} i_\beta = -\left(\frac{L_m^2 \alpha_r + L_r R_s}{\varepsilon L_m}\right) i_\beta - p \omega_r \varphi_\alpha + \frac{L_r}{L_m} V_{s\beta} + \alpha_r \varphi_\beta \end{cases} \quad (4)$$

$$\begin{cases} \frac{d}{dt} \varphi_\alpha = L_m \alpha_r i_\alpha - p \omega_r \varphi_\beta - \alpha_r \varphi_\alpha \\ \frac{d}{dt} \varphi_\beta = L_m \alpha_r i_\beta + p \omega_r \varphi_\alpha - \alpha_r \varphi_\beta \end{cases} \quad (5)$$

$$\begin{cases} T_{em} = \frac{3}{2} p \text{Im}\{\varphi_{ar} i_{\beta s} - \varphi_{\beta r} i_{as}\} \\ \dot{\omega}_r = b T_{el} - a \omega_r - f \end{cases} \quad (6)$$

where ω_r is the rotor speed, T_{em} is the electromagnetic torque, T_L is the load torque, J is the inertia, f is the viscous friction coefficient $V_{s\alpha}$, $V_{s\beta}$ are the stator voltages, i_α and i_β are the stator currents, φ_α and φ_β are rotor fluxes, R_s and R_r are the resistors of the stator and rotor, respectively, L_r , L_s are the inductances of the rotor and stator, respectively, p is the number of pole pairs, $\alpha_r = \frac{R_r}{L_r}$, and $\varepsilon = \frac{L_s L_r}{L_m} - L_m$.

To derive the proposed controller, apply uncertainties Δa , Δb , and Δf in terms a , b , and f of (6), respectively, we have:

$$\dot{\omega}_r = (b + \Delta b) T_{em} - (a + \Delta a) \omega_r - (f + \Delta f) \quad (7)$$

$$\dot{\omega}_r = b T_{em} - a \omega_r - f + d(t) \quad (8)$$

where $d(t) = (\Delta b) T_{em} - (\Delta a) \omega_r - (\Delta f)$ is the disturbance in the system. The error e is chosen as the error between the reference speed and the actual speed and is given as follows with its derivative:

$$e(t) = \omega_{ref}(t) - \omega_r(t), \quad \dot{e}(t) = \dot{\omega}_{ref}(t) - \dot{\omega}_r(t) \quad (9)$$

Based on the theory of ISMC, a new surface is chosen as follows:

$$S_1(t) = e(t) - \int_0^t \gamma e(\tau) d\tau \quad (10)$$

The derivative of the proposed surface is:

$$\dot{S}_1(t) = \dot{e}(t) - \gamma e(t) \quad (11)$$

Putting the values of $\dot{e}(t)$ from (9) in (11) we get:

$$\dot{S}_1(t) = \dot{\omega}_{ref}(t) - b T_{em} - a \dot{\omega}_r - f + d(t) - \gamma e(t) \quad (12)$$

Now to derive the ISTSMC scheme, the control law in

$$T_{eRef} = T_{eeq} + U_{ST} \quad (13)$$

The equivalent control part T_{eeq} is achieved by taking $\dot{S}_1(t) = 0$, and then the equivalent control part is given as:

$$T_{eeq} = \frac{1}{b} [a \dot{\omega}_r + f - \dot{\omega}_{ref}(t)] - \frac{d(t)}{b} \quad (14)$$

The super twisting algorithm-based control law is given as follows:

$$\begin{aligned} U_{ST} &= \frac{1}{b} \left[-\lambda_\omega |S_2(t)|^{\frac{1}{2}} \text{sign}(S_2(t)) + u_1 \right] \\ \dot{u}_1 &= -\beta_\omega \text{sign}(S_2(t)). \end{aligned} \quad (15)$$

Hence (13) can be written as follows:

$$U_{ST} = \frac{1}{b} \left[-\lambda_\omega |S_2(t)|^{\frac{1}{2}} \text{sign}(S_2(t)) - \int \beta_\omega \text{sign}(S_2(t)) \right] \quad (16)$$

the final control law from (14) is achieved by combining (15) and (16) and is given as follows:

$$T_{eRef} = \frac{1}{b} \left[a \dot{\omega}_r + f - \dot{\omega}_{ref}(t) - \lambda_\omega |S_2(t)|^{\frac{1}{2}} \text{sign}(S_2(t)) - \int \beta_\omega \text{sign}(S_2(t)) \right] - \int \gamma e(t) dt \quad (17)$$

The ISTSMC based control law fulfils the Lyapunov stability theory to ensure its stability.

3. Results and Discussion

The proposed ISTSMC control scheme was tested under normal and sudden load variations. The results showed that the ISTSMC scheme outperformed the PI control scheme in terms of overshoot, settling time, and current oscillations. The ISTSMC scheme also drew less current during load variation, which reduced the overall stress on the diodes and semiconductor switches. In addition, the ISTSMC scheme had lower power losses than the PI control scheme during load variation. These results demonstrate that the ISTSMC control scheme is a more robust and efficient alternative to the PI control scheme for motor drives.

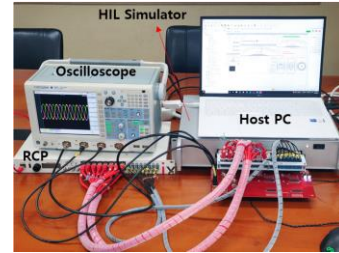


Fig. 2. Interfacing of HIL based Plant and RCP based Controller.

In the initial test, as shown in Fig. 3, the ISTSMC scheme had a 0.2 rad/s overshoot, compared to 0.4 rad/s for the PI scheme. The ISTSMC scheme also had a settling time of 0.1 sec, compared to 0.2 sec for the PI scheme.

The ISTSMC scheme also drew less current during load variation than the PI scheme as shown in Fig. 4. The peak current for the ISTSMC scheme was 1.6 A, compared to 2 A for the PI scheme. The ISTSMC scheme had lower power losses than the PI scheme during load variation. The peak power losses for the ISTSMC scheme were 1.6 W, compared to 2 W for the PI scheme as illustrated in Fig. 5. These results demonstrate that the ISTSMC control scheme is a more

robust and efficient alternative to the PI control scheme for motor drives.

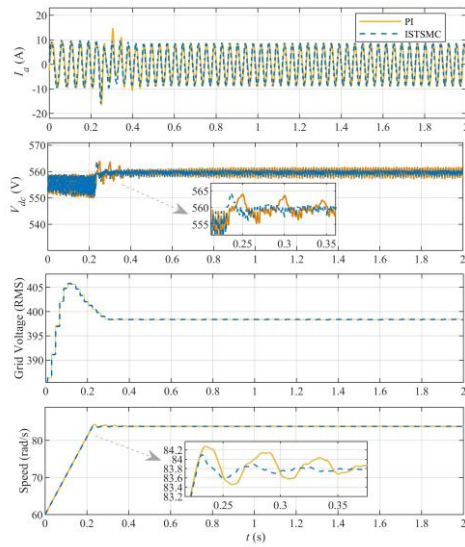


Fig. 3. PI and ISTSMC response comparison under normal conditions.

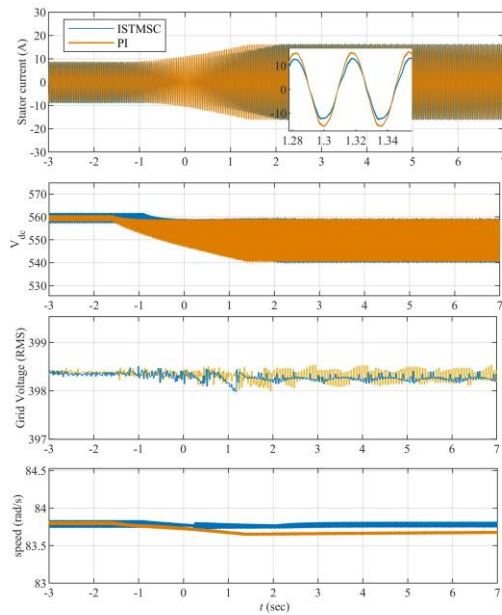


Fig.4. PI and ISTSMC response comparison under load conditions.

4. Conclusion

In this paper, we tested an ISTSMC control scheme for induction motor drive system. The ISTSMC scheme was tested in a real-time HIL environment, and it outperformed the PI control scheme in terms of overshoot, settling time, current oscillations, and power losses. It does not add any additional thermal stress to the system, and it limits the thermal stress peaks during load application. It also provides less overshoot and undershoot, and it converges to the desired speed faster. Additionally, the power losses of the

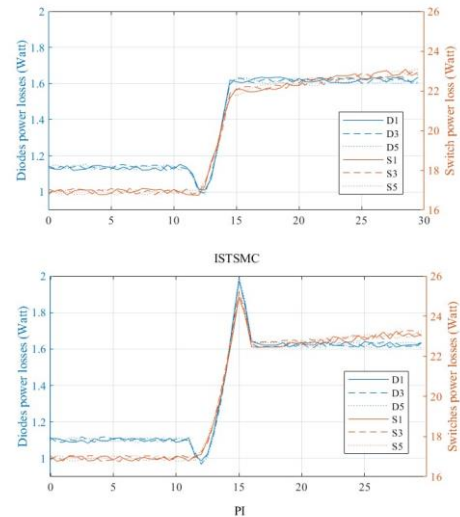


Fig.5. Diode and Switching power losses comparison (a) ISTSMC and (b) PI control scheme.

system remain constant during the loaded operation of the induction motor. It shows that by employing ISTSMC, robustness can be achieved without adding any thermal stresses to the switches while guaranteeing the same efficiency as PI control scheme.

References

- [1] M. S. Vekić, S. U. Grabić, D. P. Majstorović, I. L. Čelanović, N. L. Čelanović and V. A. Katić, "Ultralow Latency HIL Platform for Rapid Development of Complex Power Electronics Systems," in IEEE Transactions on Power Electronics, vol. 27, no. 11, pp. 4436-4444, Nov. 2012
- [2] M. N. Musarrat and A. Fekih, "A fractional order sliding mode control-based topology to improve the transient stability of wind energy systems", Int. Jour. Electric. Power Ener. Syst., vol. 133, pp. 1-12, 2021
- [3] I. Sami, S. Ullah, A. Basit, N. Ullah and J. -S. Ro, "Integral Super Twisting Sliding Mode Based Sensorless Predictive Torque Control of Induction Motor," in IEEE Access, vol. 8, pp. 186740-186755, 2020,
- [4] R. Wu et al., "A Temperature-Dependent Thermal Model of IGBT Modules Suitable for Circuit-Level Simulations," in IEEE Transactions on Industry Applications, vol. 52, no. 4, pp. 3306-3314, July-Aug. 2016, doi: 10.1109/TIA.2016.2540614